Optical Filtering with Phase Singularities

A thesis submitted in partial fulfillment of the requirement
for the degree of Bachelor of Science in Physics from
The College of William and Mary

by

William Fisher Ames

Accepted for _____
(Honors)

_____
Gina Hoatson, Director

_____
Irina Novikova

_____
Seth Aubin

_____
Hannes Schniepp

Williamsburg, VA
April 30, 2009

Abstract

I worked on constructing an optical filtering device to resolve two separate laser fields very close in frequency which are nearly collinear. It has been demonstrated to be able to achieve four order of magnitude in improvement in the resolution between two laser fields separated by less than a milliradian under ideal conditions. The size of the input fields and pinhole were optimized, and it was found that for our apparatus the field to be filtered should be 3.6 mm in diameter and wanted field to be 2.4 mm with a 0.5 mm pinhole.Such an optical filter will be applied improve the data quality of Prof. Novikova's stored light experiment, which requires two beams, one much more powerful than the other, that exit the experiment nearly collinear such that standard filtering methods are not sufficient. When applied to this experiment, the filter is demonstrated to improve resolution by two orders of magnitude under unideal conditions, and great improvement in performance is expected. The results of experiments to optimize the adjustable parameters of optical vortex coronagraph design, such as the size of the pinhole, control, and probe fields, and the topological charge of the vortex used are presented, and proposed improvements to the coronagraph design discussed.

I. Introduction

Optical filtering is the use of any technique capable of increasing the contrast between different optical fields in order to improve detection. Optical filtering techniques are important in any situation where two or more optical fields are coincident upon a detector, and one wishes to distinguish among them. The problem of distinguishing between two different fields is of great importance to atomic physics and astronomy, so optical filtering techniques have long been studied. Depending on the circumstances, incoming beams can be filtered based on frequency, polarization, spatial separation, or combinations thereof. This research is about the application of a novel spatial filtering scheme to Professor Novikova's stored light experiment.

The stored light experiment takes advantage of long-lived spin coherence in atoms to create electromagnetically induced transparency using a Rubidium vapor cell. The electromagnetically induced transparency in turn stores light by dramatically reducing the group velocity of light within the Rubidium gas. This effect requires two input

lasers. The control field, which creates strong coupling between the light and the atoms, and probe field, which is the stored field. To create stored light the frequency between these fields is 6.8 GHz. To avoid Doppler broadening of the two-photon transition, the control and probe fields must be kept as close to collinear as possible. The detection poses an additional problem, since we wish to detect only the probe field, and completely eliminate the control field which can be many orders of magnitude more intense. The frequency difference between the fields is sufficiently small that frequency filtering techniques are not sufficiently effective, and the difference in intensities is such that even after filtering with polarization, the control field overwhelms the probe field. In order to make the probe field detectable, the beams are made to propagate with a small angle between them. While this makes it possible to discern them with the detector, it reduced the quality of light storage. The goal of this project was to develop an optical filter capable of separating two fields at smaller angle. A separation between the beams would still be necessary, but the filter would allow this angle to be reduced. Because of the requirements of the stored light experiment, the filter must not require any changes to the frequency or polarization of the input fields, nor can the radius of the probe field be greater than that of the control field. The objective is to minimize the resolvable angle between the beams. It was decided that the best way to do this is with an optical vortex coronagraph.

This paper begins with a discussion of the stored light experiment, so as to clarify the necessity for spatial filtering and the restrictions placed upon the design parameters. Second, it discusses the principle of operation of the Lyot stop coronagraph, upon which the design of the optical vortex coronagraph is based, as well as the properties

and creation of optical vortices. Third, it will discuss the optical vortex coronagraph itself: its design, theoretical performance, and the construction of a prototype for parameter optimization. After a discussion of the methods used to determine the ideal coronagraph parameters and their results, we will move on to the final vortex design, the installation of the optical vortex coronagraph onto the stored light experiment, and proposals for further improvements to the design.

II. Stored Light Experiment

The stored light experiment is based on the concept of electromagnetically induced transparency, or EIT, in a hot Rubidium gas. The Rubidium atoms have a lambda energy level structure, shown as Figure 1. Two laser fields are shone into the Rubidium; the control field is resonant with the |b> to |a> transition, and the probe field with the |c> to |b> transition. It can be shown [1] that so long as both fields are kept in phase, and the difference in their frequencies corresponds to the difference between the |b> and |c> energy levels, the |a> level will not be populated; there will be no transitions to or from the |a> energy level. As a consequence, the absorption of light of wavelengths resonant with |a> transitions drops to 0, resulting in a large and rapid change in the absorption versus frequency of incident light, as shown in Figure 2.

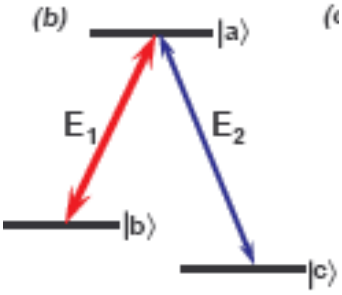

FIGURE 1: Diagram of the lambda system, with the control field in red and probe field in blue. Image from [1].

As index of refraction varies directly with absorption, this implies there is also a large and rapid change in index of refraction. Most importantly, group velocity of light in a medium is directly related with the derivative of the index of refraction with respect

to wavelength in the medium. Therefore, at the zero of absorption the group velocity of light is extremely low. It is this very low group velocity which results in slow light and light storage: it takes a long time for the photons to make it across the Rubidium gas cell.

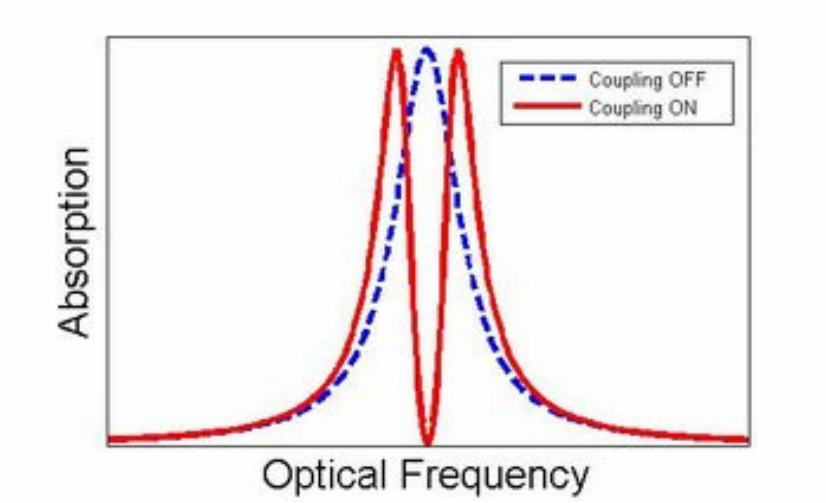

FIGURE 2: Absorption versus frequency under normal conditions (blue) and under EIT (red). Image from [11]

In order to maintain EIT, the frequency difference between the control and probe field must be kept extremely close to the |b> and |c> transition in the Rubidium. Unfortunately, as the Rubidium is a gas, the atoms in it are moving, and any velocity component not orthogonal to the incoming beams results in a Doppler shift. This Doppler shift will change the frequency difference between the two beams unless they are exactly collinear. The Doppler shift is

$$f = \left(1 - \frac{v}{c}\right) f_0 \qquad (1)$$

Where f is observed frequency, f_o is the source frequency, v is the velocity of the observer, and c is the speed of light. It is due to this consideration that we wish to get the probe and control fields as close together as possible. From this we can see that the difference in frequency between two fields propagating collinearly

$$\Delta f = \left(1 - \frac{v}{c}\right) f_0 - \left(1 - \frac{v}{c}\right) f_1 \qquad (2)$$

Where if is the frequency of the second field. Since f_1 is close in frequency to f_0, the change in frequency is close to 0. Further, any probe field light that is not coincident in the gas cell with control field light does not see transparent gas, which means no light storage. Therefore, we also do not want a probe field large in diameter than the control field.

III. Lyot Stop Coronagraph

The problem of distinguishing between two light sources very near to each other with one many orders of magnitude brighter than the other is one which was first treated by Bernard Lyot in 1930 and used extensively since by astronomers. (2) Lyot developed his coronagraph as a tool to observe the solar corona, from which coronagraphs derive their name. A diagram of , the Lyot stop coronagraph, which is the basis of the optical vortex coronagraph, can be seen in Figure 3. The two beams of light, one of

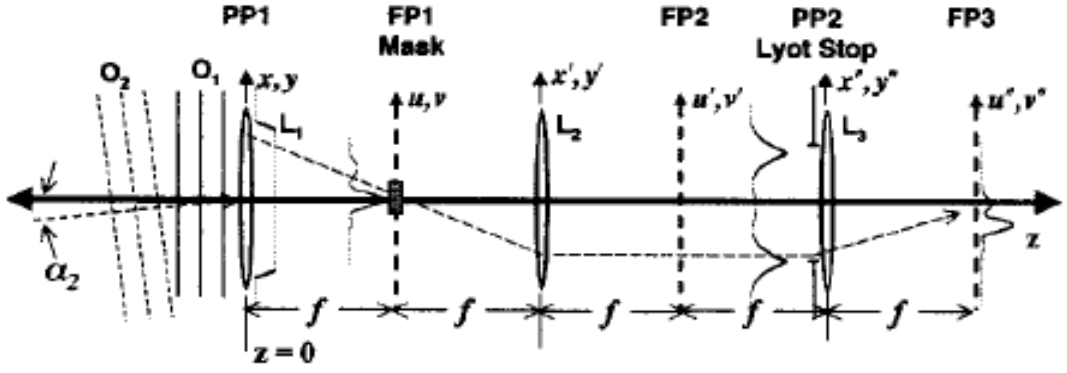

FIGURE 3: Lyot Stop Coronagraph: The two input beams enter from the left, enter lens L1, and are focused to FP1. The occulting mask on FP1 block the unwanted field, the other propagates through to L2, which recollimates it. PP2 is image processing and focusing onto a detector at FP3. [1]

which we wish to observe, and the other, brighter beam which we wish to eliminate, enter the coronagraph from the left. The first lens focuses each of the beams to a different point on the focal plane. An occulting mask, which is essentially a black object, is placed in front of the unwanted beam, which is absorbed. The desired beam propagates past the occulting mask unaffected before being recollimated by the second lens. So long as the two beams are focused to separate, distinguishable points, this filter allows the observation of the desired optical field with minimal light loss while nearly completely blocking the other beam.

Unfortunately, in some cases the Lyot stop coronagraph is not perfectly effective. Due to diffraction, the first lens does not focus incoming light beams to points, but rather to finite disks on the focal plane. Should these disks, known as Airy disks, overlap, the Lyot stop coronagraph can no longer resolve the objects, as it is impossible to eliminate all of the unwanted light field without also compromising some of the desired one. If the overlap is sufficiently large, or the unwanted field sufficiently bright, it makes distinguishing between the two fields impossible. For such situations, a different filtering scheme is required. In our case, we elected to use an optical vortex coronagraph.

IV General Properties of Optical Vortices

An optical vortex, also known as a phase singularity or screw dislocation, [1] is a zero of optical field intensity within an otherwise non-zero field. The field amplitude of a beam carrying an optical vortex, more properly known as a Laguerre-Gaussian beam, can be described as a composition of a Gaussian function with Laguerre polynomials.

$$E = \left(\frac{r}{w_0} \right)^m e^{-r^2/w_0^2} e^{im\vartheta} e^{ikz - i\omega t} \qquad (3)$$

Where E is electric field, ω is angular frequency, w_0 is the beam waist, r, φ, and z cylindrical coordinates, and m is an integer constant. This constant, known as the "topological charge," is the number of periods in one rotation about the axis. It can be thought of as the rate at which the phase spirals about the axis. A picture of an optical vortex beam, taken during the course of this research, is shown as Figure 4. For comparison we show a Gaussian field in Figure 5. An optical vortex is formed when a beam of light, instead of having constant phase across a wave front the way we normally imagine a light beam, has a phase which spirals about a central axis, forming a helix. At the central axis, all light destructively interferes, forming the optical vortex.

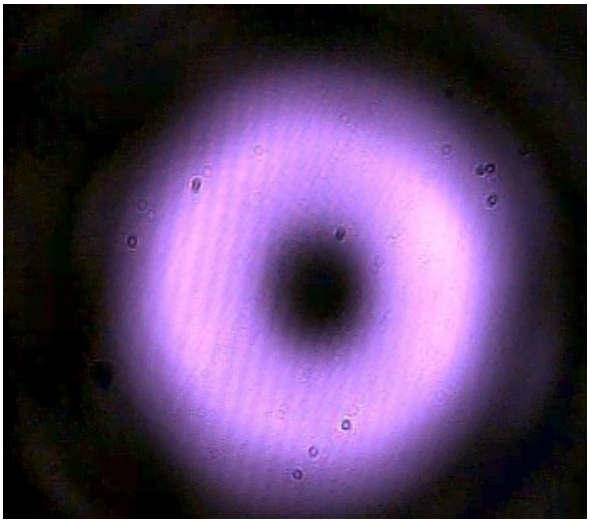

FIGURE 4: Optical vortex beam made in our lab using optical vortex phase mask, with light from optical fiber. The vortex is the dark spot in the center. The laser is infrared, the camera's color scale labels infrared with purple.

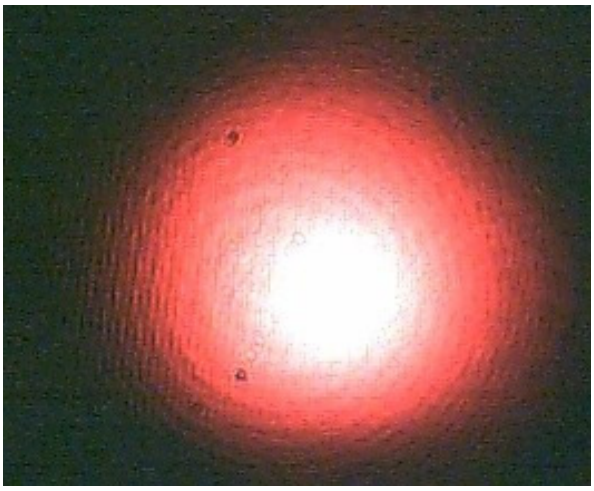

FIGURE 5: Near-Gaussian beam, what the laser field from a diode laser looks like before passing through the vortex phase mask and becoming an optical vortex beam.

Optical vortex beams have many interesting properties, such as the ability to carry angular momentum, and many

proposed uses, such as optical tweezing. [10] However, for this research, all that is important is that they have a dark spot in the center and a donut shaped intensity profile.

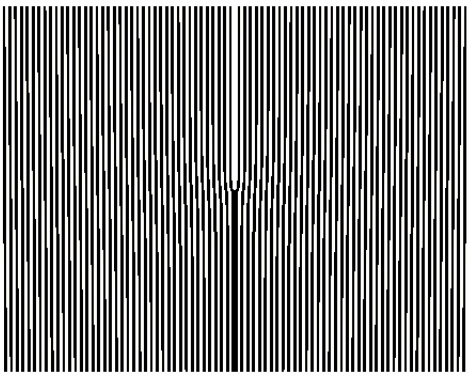

FIGURE 6: A homemade hologram used to make optical vortices. Notice the fork in the center.

V. Creation of Optical Vortices

There are three primary ways to create optical vortex beams [1] [3] [6], of which two were used during the course of this research. Optical vortex beams have been created using diffractive optics, [3] however, while a Laguerre-Gaussian beam keeps its shape as it propagates, vortices created with diffractive optics do not. This makes them difficult to apply to our application. The other two methods are to use holograms and optical vortex phase masks.

The first optical vortex beams created in our lab used a hologram similar to the one shown as Figure 6. It looks much like a standard diffraction grating, except there is a fork in the middle of the grating. It is this fork which creates the vortex beams, and the more tines on the fork, the greater the topological charge of the output beams. The hologram is created by calculating the interference pattern of an optical vortex beam, using Equation 3, with a Gaussian beam, such as the one shown in Equation 4.

$$E(r,z) = E_0 \frac{w_0}{w(z)} e^{-r^2/w(z)^2} e^{-i(kz - \arctan(z/z_R) + kr^2/(2R(z)))} \quad (4)$$

Where w(z) is a function defining variations in beam waste, z_R is the Rayleigh length and is equal to pi times the beam waist width squared over the wavelength, and $R(z)=z[1+(z_R/z)^2]$. The result is the hologram shown as Figure 7.

These calculations were performed with Matlab, though any computational software should suffice. One then needs to convert the calculated interference pattern into a hologram. The best way to do this in Matlab is to set the output to grayscale with only two possible color values, completely black and completely white; dividing the range in half between them. At this point, the greatest difficulty is in producing the hologram at sufficient resolution to be usable. Typically printers do not have sufficient resolution to produce a hologram capable of creating and optical vortex beam, however, many photocopiers do. So I printed out the hologram four times the size (twice as big in each dimension) as is actually desirable, and then use the copy and shrink function on the photocopier to reduce it to the desired size onto a transparency. Note that when printing the hologram, it is important to be able to control the physical dimensions of the hologram on the page.

The home-made holograms produce vortex beams which are not of particularly high quality. However, they do produce many different beams, each of a different charge: the topological charge of a particular vortex is equal to the order of the diffraction maximum it is in. Such a set of vortex beams produced by a hologram can be seen as Figure 7. Individual first and second order vortices produced by hologram in our lab can also be seen in Figure 7. A hologram on loan from us from Dr. Carlos Lopez-Mariscal produces much cleaner vortices than our homemade ones did, as it was created using a dark room and photographic methods, with which I am not familiar. While the

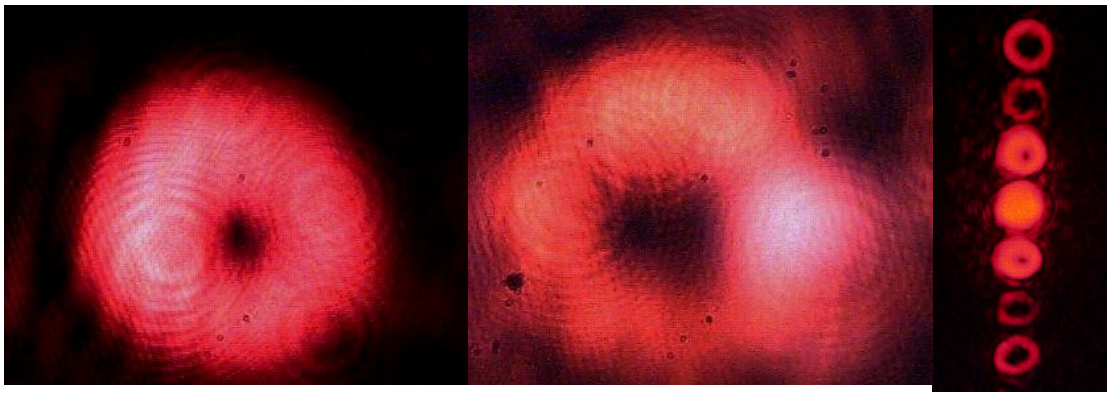

FIGURE 7: Left: First order optical vortex generated by hologram in our lab. Center: Optical vortices made by hologram. Center maximum is a Gaussian beam, next are vortices of charge +1 and –1, then +2 and –2, with +3 and –3 on the outside. Left: Second order optical vortex generated by

hologram was not useful for filtering, due to the fact that it splits incoming beams into multiple output beams, it was the only method available to us for a time, and was useful for learning to identify vortices and becoming familiar with their behavior in the laboratory.

To create the optical vortex beams used in our filter we used an optical vortex phase mask. The standard optical vortex phase mask is a piece of glass carved into a sort of spiral staircase shape. An example is shown as Figure 8. Each of the wedges of the spiral staircase applies a different phase shift to the transmitted Gaussian beam. Around the entire circumference of the staircase, an integer multiple of 2π phase shift is applied. This integer multiple of 2π is the topological charge of the created vortex, m. The result is an optical vortex beam, such as the ones shown as Figure 4, created in our lab using the optical vortex phase mask on loan to us from Dr. Grover Swartzlander. We used optical vortex beams of topological charge 1.

What actually creates the vortex in the vortex beam when using the phase mask is the central point where all the glass wedges come together, and light with all different phases interferes destructively. If the incident beam does not overlap this central point,

no vortex is created. This is what allows the optical vortex coronagraph to surpass the Lyot stop coronagraph in quality. The occulting mask of the Lyot coronagraph must completely block the control field, while affecting a minimum of the probe field, while the optical vortex coronagraph can turn the control field into a vortex and filter it so long as its center is aligned with the center point of the phase mask, while the probe field can pass unaffected so long as it does not intersect the single point at the center of the phase mask [2].

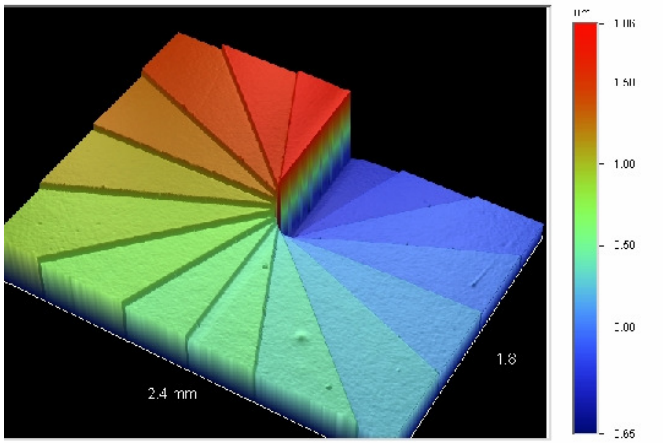

FIGURE 8: Optical Vortex Phase Mask. Note the center piece where each of the glass wedges join together. It is this point which creates the vortex. Image from: www.u.arizona.edu/~grovers/ovc/002.jpg

VI. Testing of Optical Vortices

One can determine if an observed dark spot in the beam is actually from an optical vortex beam, and not some diffraction artifact, by interfering the suspected optical vortex beam with a Gaussian beam in an interferometer: the output should look the same as the hologram used to create the vortex. We performed this testing using a combined Mach-Zehnder and Sagnac interferometer, which is discussed in detail elsewhere. [9] Note that the Sagnac effect is not necessary for this experiment, there is merely a similarity in design. The design of this interferometer is shown as Figure 9. We used this technique when first creating vortices in order to make sure that we were actually generating vortices, and not seeing a diffraction or scattering effect due to an imperfection in or piece of dust on the hologram or one of the optics, since low quality vortices are diffi-

cult to distinguish from such effects.

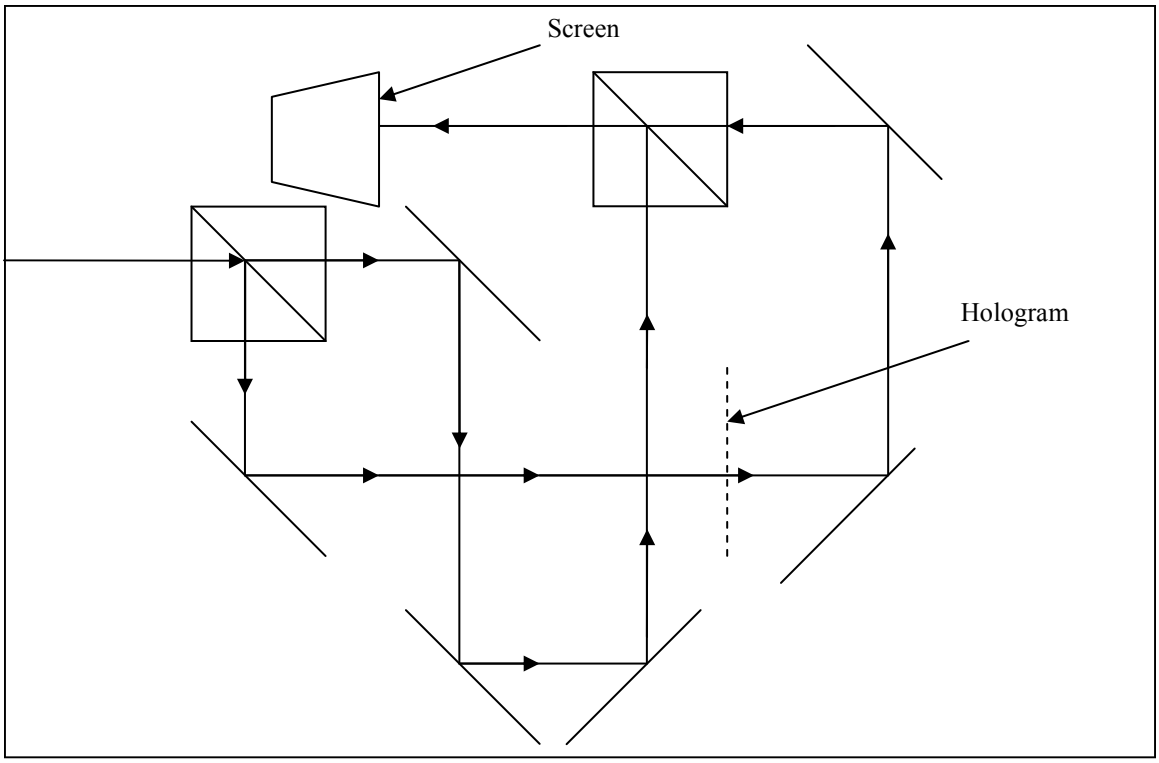

FIGURE 9: Design of a modified Mach-Zehnder interferometer. The purpose of the two cavities is so that no light passes through the hologram more than once, which would complicate the results. Note that

VII. The Optical Vortex Coronagraph

We achieve the desired filtering using the optical vortex coronagraph, designed by Dr. Swartzlander in order to directly observe exoplanets. [1] A diagram of its design is shown in Figure 9. The optical vortex coronagraph is very similar in operation to the Lyot stop coronagraph. Like the Lyot coronagraph, the first lens focuses each of the beams to an Airy disk slightly offset from each other. However, instead of an occulting mask placed in front of the unwanted beam, an optical vortex phase mask is used instead. The optical vortex phase mask turns the unwanted beam into an optical vortex

beam, as the unwanted beam passes through that vital center point, while the probe field, the beam we wish to keep, does not pass through that central point, and thus is not affected. A second lens then recollimates both beams. Note that running an optical vortex beam through a lens does not destroy the vortex. As we shall see later, vortices are resilient under a surprising variety of optical transforms. After both beams are recollimated, a pinhole is placed in front of the beams, with the hole chosen such that it blocks as much of the offending light field as possible, while allowing most of the desired field to pass through unmolested. It is this pinhole which performs the actual filtering operation.

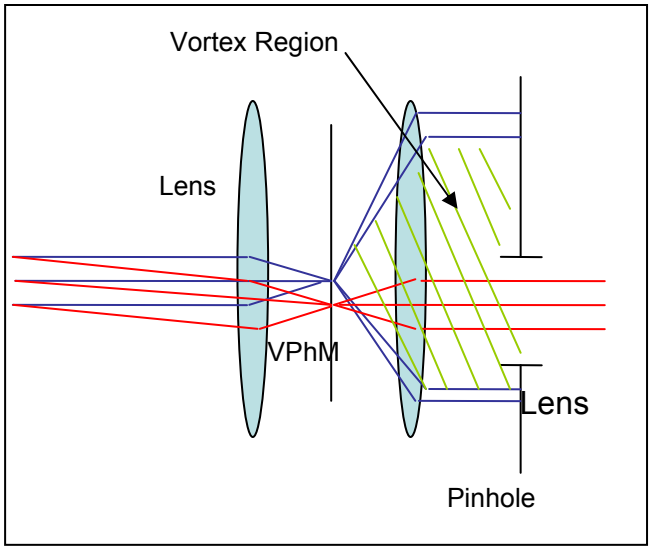

FIGURE 10: Optical vortex coronagraph design. The control field (blue) and probe field (red) enter from the left with a small (greatly exaggerated) angle between them. The first lens focuses them onto the plane of the vortex phase mask. The control field sees the center point of the vortex phase mask, becoming an optical vortex, while the probe field does not. They are recollimated by the second lens, and the pinhole blocks the vortex beam, as it is open only in the dark region of the vortex, but he Gaussian probe field passes through. Note that while the probe field does pass through the optical vortex phase mask, it does not pass through its center, and as a consequence does not become a vortex beam. Its phase structure is changed, but not in a fashion which effects its intensity profile.

In designing an optical vortex coronagraph for a particular application, there are several parameters which need to be fixed. These are the size of the pinhole, the size of the input beams, , and the angle between the beams at input. We had little control over the size of the pinhole, only having two pinholes, one of 500 micrometer diameter, the other 150 micrometer diameter. However, the actual size of the pinhole is not as important as the size of the pinhole compared to those of the control and probe fields, so by

careful selection of the control and probe field sizes, we can compensate for the lack of choice in pinhole size. The angle between the input beams is the quantity we are attempting to minimize, so the input beam angle will be set to the smallest possible angle that will still allow the two beams to be distinguished. The only other variable is the topological charge of the vortex. While variable in principle, we only have a charge 1 optical vortex phase mask. Therefore, the most important design task was determining the ideal beam sizes and which pinhole to use.

VIII. Theoretical Maximum Performance of the Optical Vortex Coronagraph

The theoretical maximum possible performance of the optical vortex coronagraph was presented by Swartzlander [1]. This paper predicts that the optical vortex coronagraph would have perfect filtering efficiency: completely eliminating the control field while allowing the probe field to propagate through unaffected for beams separated by an angle equal to $0.61\lambda/R_{EP}$, where R_{EP} is the entrance pupil size, the smallest angle resolvable with a Lyot stop coronagraph [1]. Unfortunately, the paper makes a critical simplifying assumption which my subsequent work has shown to be inapplicable to filter construction, and even with that assumption in place, the remaining mathematics, while technically correct, is not particularly applicable to the actual construction of an optical vortex coronagraph. In essence, the authors state that the optical vortex coronagraph can achieve perfect filtering if the pinhole used is as small as the zero-intensity region of the vortex, and the probe field fits entirely within the pinhole. However, Equation 1 shows that the actual region of zero intensity in the optical vortex is infi-

nitely small, therefore, while the paper's derivation is correct, the conditions under which it is valid, namely, an infinitely small probe field and an infinitely small pinhole, are somewhat impractical in a laboratory. Therefore, I had no useful theoretical prediction of the maximum filtering capability of the optical vortex coronagraph available to me.

Accordingly, I set out to try to complete this calculation myself. I defined an ideal filtering radius, which is the radius projected onto the plane of the detector in which the intensity of the probe field is equal to intensity of the control field. In the area inside this radius, the probe field is more intense than the control field, and therefore we wish to allow that region to pass, while in the region outside the ideal filtering radius, the control field is brighter than the probe field, and is therefore the area we wish to filter out, a shown in Figure 11. Unfortunately, this is not a simple matter of graphing the intensity profiles of an optical vortex beam and a Gaussian beam of the correct parame-

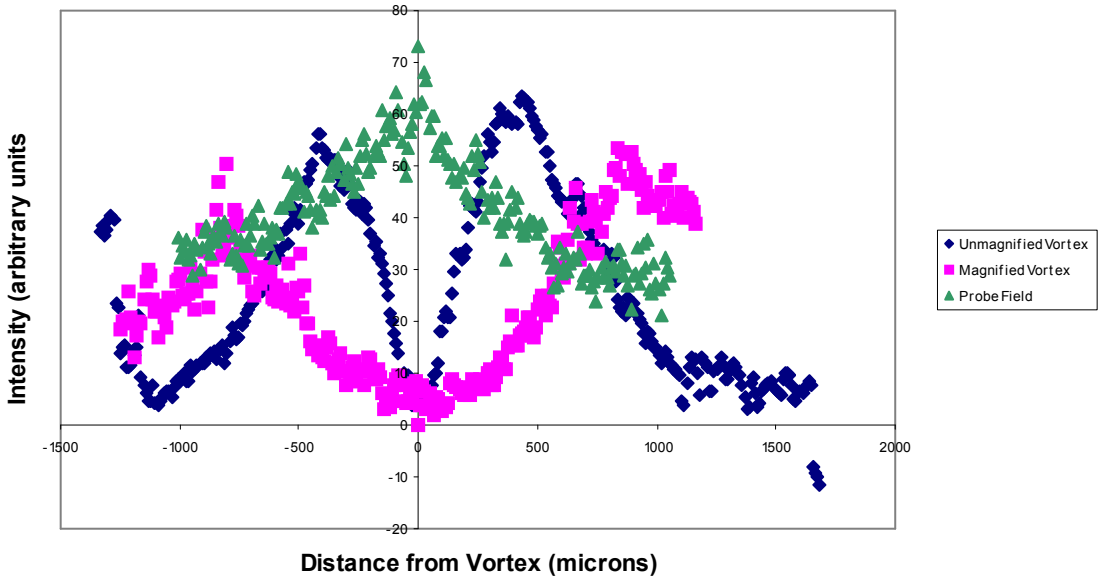

FIGURE 11: Ideal filtering radii for a magnified and unmagnified vortices. The intersections of each vortex with the probe field defines the ideal filtering radius for the respective vortex beams.

ters and determining where the curves cross, as there is significant diffraction caused by the pinhole. In particular, significant light from the control field is diffracted from outside the pinhole inside, which causes problems. In essence, the problem of determining the ideal filtering of the optical vortex coronagraph for given beam intensities and geometries reduces to the problem of calculating diffraction of an optical vortex through a pinhole. There are two approximations used in calculating diffraction, the Fresnel, or near-field, and the Fraunhofer, or far-field. As a rule, the far-field approximation can be used when the Fresnel number is much less then one, where the Fresnel number, F, is given by Equation 5.

$$F = \frac{a^2}{L\lambda} \tag{5}$$

Where a is the radius of the aperture, L is the distance from the aperture to the screen/detector, and λ is the wavelength. For all probable designs of the filter, aperture size is on the order of hundreds of micrometers, distance between the aperture and the detector is on the order of centimeters, and wavelength is in hundreds of nanometers, so clearly F<<1, and the Fraunhofer approximation can be used.

The Fraunhofer diffraction equation outputs a function $U_i(x,y)$ in terms of position on the image plane, when given a function in terms of position on the diffracting aperture plane $U_d(\xi,\eta)$.

$$U_i(x,y) = \frac{e^{ikz} e^{i\frac{k}{2z}(x^2+y^2)}}{i\lambda z} \iint U_f(\xi,\eta) e^{-i\frac{2\pi}{\lambda z}(x\xi+y\eta)} d\xi d\eta \tag{6}$$

Where x and y are position on the image plane, ξ and η are position on the aperture plane, and z is the distance between the two planes. U(ξ,η) is the distribution at the plane of the aperture. The integration is performed across the surface of the aperture. Converting the aperture plane coordinates into polar coordinates r and φ, this results in the following equation in the case of a Laguerre-Gaussian beam:

$$U_i(x,y) = \frac{e^{ikz} e^{i\frac{k}{2z}(x^2+y^2)}}{i\lambda z} \iint \left(\frac{r}{w_0}\right)^m e^{-r^2/w_0^2} e^{im\vartheta} e^{ikz - i\omega t} e^{i\frac{2\pi}{\lambda z}(xr\cos\vartheta + yr\sin\vartheta)} r dr d\vartheta \tag{7}$$

Unfortunately, actually solving this integral is quite difficult, in fact, it is analytically impossible. Numerical integration routines do not converge. In response, I tried several approximations of this integral. The first, a pair of Taylor series, one in r and the other in φ, were poor approximations of the actual function. In response, I broke up the r-portion into 10 different areas, did a Taylor series about each of these segments, and created a piecewise function which was an excellent approximation of the amplitude distribution. To deal with the rest of the function, I tried to construct a Fourier series in terms of φ, but that could not be calculated in reasonable time. Out of ideas, I put these calculations on hold, and we have resolved to solve the problem experimentally.

IX. Prototype Apparatus

In order to test the performance of the optical vortex coronagraph, and as a starting point for testing improvements, I constructed a prototype optical vortex corona-

graph, using a HeNe laser and red diode laser combined with a beam splitter to represent the control and probe fields, respectively. A schematic of the prototype can be seen as Figure 12. After being combined at the beam splitter, which is placed on a rotary stage to allow the angle between the beams to be changed, the fields propagate to a lens, which focuses them to the phase mask. They then pass through a collimating lens, before arriving at the pinhole. The pinhole filters the beams, and from there the light arrives at a CCD web camera, with appropriate filters. The optical vortex phase mask is placed on a translation stage, which, in addition to helping with alignment, allows the phase mask to be removed from the apparatus.

Data acquisition and analysis is performed by taking a series of photographs, one of the probe field and vortex with the pinhole in place, which is the filtered output; a second with the vortex and the pinhole, in order to measure the intensity of control field light that is filtered; then a third with the probe and the pinhole, to measure the intensity of probe field light passed by the filter. A picture of the control field by itself without the vortex or pinhole is taken, so as to determine the intensity of control field light with

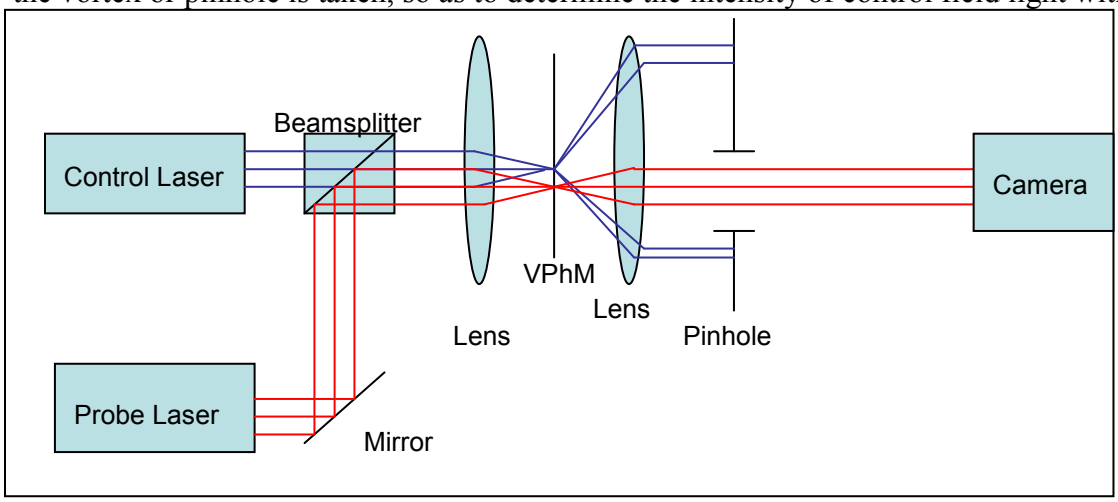

FIGURE 12: Apparatus used in exploring various parameters of the optical vortex coronagraph. Note that the input fields are provided by combining two lasers with a beam splitter. Additional optics could be places between any two components of the prototype except between the vortex phase mask and the two lenses next to it. The vortex phase mask was mounted on a translation stage to allow it to

no filtering; then the probe field by itself without the pinhole, in order to measure the intensity of the probe field without any filtering; and last a picture of both the control field and the probe field, which shows output without any filtering. Finally, I took pictures with no lasers on at all for each level of filtering I used during the experiment as background measurements. I analyzed this data by using ImageJ, an image processing software freely available online. From each picture I subtracted the dark picture of the same filter level. I then used ImageJ to add up the total amount of light in a circle encompassing the beam on the picture: it produced an average light level over an area, and the area of the selection. I then multiplied these two values together. As an additional dark current control, I then selected a small circle of black in a corner, and get the same statistics. I then multiplied the average pixel value in the black region by the area of the region of interest, and subtracted that from the total amount of light in the region of interest. I tested the reliability of this method of background control by comparing the values found using different sizes of circle around the regions of interest, and found that all of the numbers in the data are accurate to 20%. I measured the performance of the coronagraph using the methods outlined above with a 500 micron pinhole installed, and then again with a 150 micron pinhole installed. The 500 micron pinhole resulted in reducing the intensity of the control field by a factor of 5.2 and the probe field by 1.5 Use of the 150 micron pinhole resulted in a reduction in intensity by a factor of 880 and the probe field by a factor of 40. These were done with 1.8 mm diameter control field. The probe field had an average diameter of 1.16 mm

X. Determination of Ideal Beam Sizes

The optical vortex coronagraph was originally designed for astronomical applications, where there is little or no control over the input to a filter. Since our input comes from a tabletop atomic physics experiment, we have a much greater degree of control over the incoming light. The intensity of the light is determined by the needs of the slow light experiment, the probe field cannot be greater in diameter than the probe field, and, of course, bringing the beams as close to collinear as possible is the objective of the research. Changing the radii of the light fields, in particular, was an attractive avenue to explore. Clearly, a larger dark area in the optical vortex field would be quite beneficial to the efficacy of the filter, while a smaller probe field would get more of its light through the pinhole. We purchased an adjustable magnification telescope in order to investigate this.

The telescope had a nominal magnification range from 2 times to 5 times, however, there was no scale on the device. Using a micrometer, I drew lines of width equal to integer and half-integer multiples of the input beam width from 2 to 5, and adjusted the telescope until the output beams were the same diameter as the lines I had drawn, and marking the appropriate position on the ring. I first used the telescope to find the effect of increasing the radius of the probe field on filtering efficiency, and quickly determined that it had the expected effect of reducing the effectiveness of the filter, as with a wider beam less light made it through the pinhole. Since a wider probe field would be undesirable for both the slow light experiment and the filter, I spent no further time in that investigation. Since shrinking the control field radius should reduce filtering effi-

ciency, as more of the control field fits through the pinhole, as well as affecting the performance of the stored light experiment, I did not experiment with decreasing the control field size.

I then used the telescope to find the effects of a larger control field. I found that a larger diameter control field results in a larger diameter vortex, which greatly improves the quality of the filter, with control field attenuation as high as a factor of 5.6×10^4, much better than the 8.8×10^2 seen without control field magnification. I then tried to determine the consequences of shrinking the radius of the probe field. Due to the poor beam quality of the laser used to represent the probe field, I was not able to use a telescope to reduce the diameter of the beam. Instead, I placed a 750 mm focal length lens in front of the probe field, but before the beam splitter that combines the two beams. The pinhole was placed at the focal plane of the lens, so that the lens effectively shrank the probe field on the plane of the pinhole, which is really what we needed. Using this arrangement in tandem with the expanded control field, I have achieved control field attenuation of 5.6×10^4 and probe field attenuation of 28, yielding an improvement in contrast between the two beams by a factor of 2000 over no filtering. By using a different laser for the probe field, one with a higher beam quality and thus a tighter focus, this was improved to control field attenuation of 4.39×10^4 and probe field attenuation of 4.6, or an improvement in contrast by a factor of 9500 over no filtering.

Having determined that the size of the vortex can be increased by magnifying the optical vortex beam, and that the increased vortex size and decreased probe field size dramatically improve filtering effectiveness, we sought to determine what the ideal beam sizes would be for a given vortex size. The ideal filtering radius I had been work-

ing with up until this point was no longer well defined; I needed a new definition of the size of the vortex region that would be independent of any external reference beam. Since the intensity of the control field would be many orders of magnitude greater than that of the probe field, we would likely only want the very darkest part of the vortex. While selecting the region where the control field intensity is zero would result in the same impracticality problems as Professor Swartzlander's calculation, it would be possible to select an area where control field intensity is *indistinguishable* from zero: areas where the measured intensity within the vortex is less than the average background. I measured this radius for each integer and half integer magnification level from 2 to 4.5, as well as with no magnification at all, by running light from an optical fiber through the telescope, then shining it on the vortex phase mask, and taking a picture of the output with the camera. After background correction, I then recorded the intensity values of points from two profiles of each picture, one horizontal, one vertical. These were averaged together to get a mean intensity versus distance from vortex graph, and the radius from the center of the vortex which is indistinguishable from background recorded. The results of this can be seen graphed as Figure 13. The graph seemed to be a nice corroboration of the previous determination that a magnified beam results in a magnified vortex, as it is quite linear.

Despite the appearances of Figure 13, it was not yet clear what size of input field we would like to use, as there are practical reasons that a large control field is difficult to work with. At the larger magnifications, the size of the beam is very close to the size of the lenses in the filter, which makes alignment much more difficult and frequently results in very noticeable diffraction fringes in the output. In the hopes of finding a use-

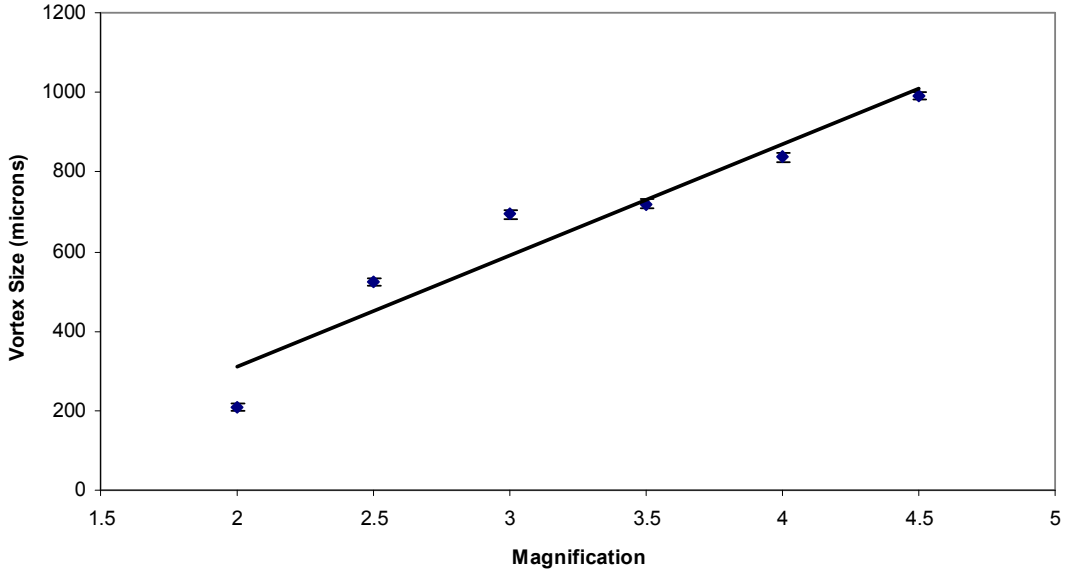

FIGURE 13: Size of region of vortex indistinguishable from background versus magnification. The plot behaves in a linear fashion, which is heartening and useful from an optical design standpoint.

ful middle ground, I measured the amount of light the 500 micron pinhole allowed through from vortices under each level of magnification. The results are graphed as Figure 14; note the logarithmic scale. The fact that little gain in filtering is made after 3x magnification, and that the beam width starts becoming difficult to work with at 3.5x makes the 3x magnification field the clear preference. This allowed us to determine the ideal control beam size to be 3.6 mm.

From here, the determination of ideal probe field input radius was similar. We want the probe field to be as small as possible. Since we use a lens to focus the light of the probe field through the pinhole, we want the Airy disk to be as small as possible. The size of the Airy disk gets smaller as aperture size gets larger assuming no aberrations, therefore it is beneficial to send a *larger* probe field through the focusing lens, assuming a high-quality lens. Since we do not want the probe field being any larger than the control field, this set the ideal probe field size as the same as that of the control field.

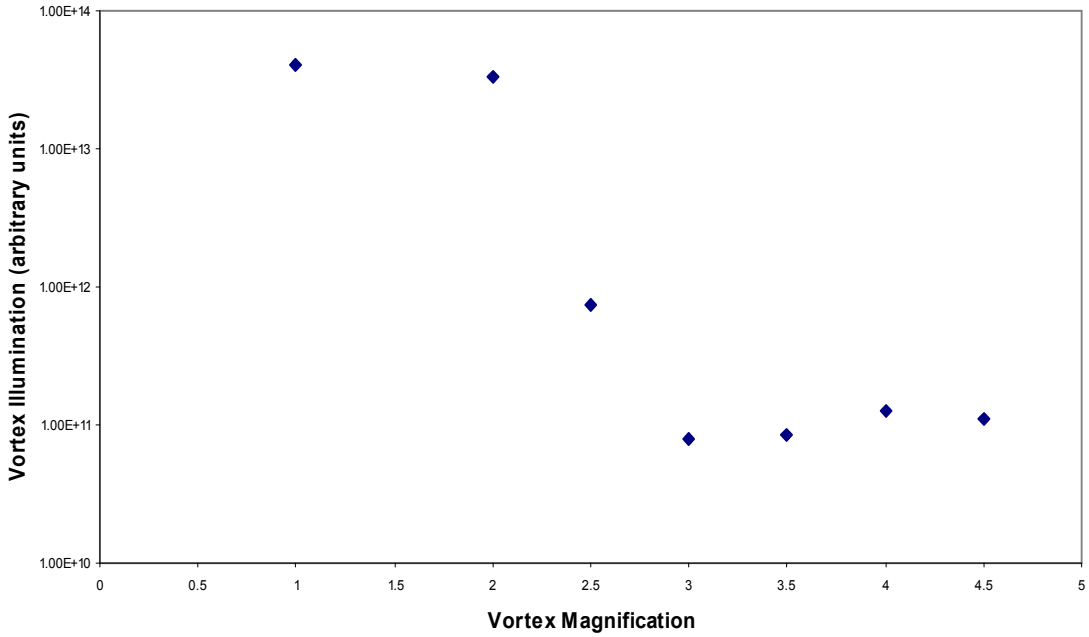

FIGURE 14: Illumination passed through pinhole for varying sizes of vortex. Note the logarithmic scale. The turning point at magnification= x3 is the key point, past which there is minimal gain in filtering for an

Experimentation, performed by magnifying the probe field with the telescope before it is sent through the focusing lens, however, showed that while there was significant benefit to filtering efficiency from doubling the size of the probe field, the benefit dropped off and eventually decreased. Perhaps the drop in benefit is due to the fact that the telescope, since it is adjustable, likely does not output collimated light, which would reduce the quality of the focus.

XI. Installation of the Optical Vortex Coronagraph

The optical vortex coronagraph is currently being installed on the stored light experiment. The stored light experiment needed to be moved and realigned so as to allow room for the optical vortex coronagraph, the lens which will need to be placed within the stored light experiment to focus the probe field, and so that the beam sizes

could be manipulated. Preliminary results, with no modifications of the beam size, leaving it at approximately 3 mm for both the control and probe fields, and the 150 micron pinhole resulted in a filtering factor of 2.4×10^5 for the control field and 1.2×10^3 for the probe field, for an overall improvement in resolution by better than a factor of 190. With properly adjusted beam sizes, it is expected to be able to perform better.

XII. Holograms and High Order Vortices

Dr. Swartzlander suggests using a second order vortex instead of a first order vortex for filtering, as the second order vortex beam's dark region is larger [1]. Currently we have no phase mask capable for producing higher order vortices, but we did have a high quality hologram for test measurements.

We used a hologram from Dr. Carlos Lopez-Mariscal at NIST in order to test this, as my home-made holograms were not of high enough quality. I modified the apparatus to place the hologram after the phase plate but before the pinhole. The spiral phase plate can be disengaged by moving the translation stage, and the hologram was installed on a flip mount, so it could be engaged and disengaged as needed. Initially, I put a focusing lens before the hologram and a collimating lens after it, similar to the spiral phase plate, but I did not manage to get any vortices this way. I suspect that the Airy disk of the beam is too small to get the necessary interference to produce the hologram, though it is possibly that I just never got the focal point over the fork of the hologram: the lines of the hologram are nearly invisible and extremely close together, making it impossible to see the fork in the hologram which creates the vortex. Without the lenses, it is fairly simple to find the vortex and line up the pinhole, so all data I took was with-

out any focusing on the hologram. The hologram produced three maxima of intensity bright enough to be useful. The zeroth order maximum was a Gaussian field, the first order to the right was a first order vortex, the second maximum was a second order vortex, and the vortices to the left of the zeroth order maximum were negative order vortices. I compared the first and second order vortex filtering efficiencies. I lined up the pinhole with the maximum I wished to investigate, and took the same collection of pictures as with the optical vortex phase mask. Note that the probe field "sees" the hologram as just a diffraction grating, as it does not go through the fork, so it is split up into the same maxima, but none of the fringes are Gaussian beams. For filtering with the first order vortex from the hologram, I found the control field to be attenuated by a factor of 2.83 and the probe field by 2.94. For the second order vortex, I found the control field to be attenuated by a factor of 33.3 and the probe field by 4.1.

Clearly, the second order vortex provided better results than the first order, but there are other factors to consider. Less light goes into the second order fringes than the first order, and the "unfiltered" pictures were taken with the hologram removed entirely, so that effect must be controlled for. The probe field, however, has the same issue: the order of probe field used was always the same as the order of control field. Given that the difference between the first and second order probe fields is ~36%, and the difference between the second and third order control field attenuations is over 1000%, it seems highly unlikely that the difference in the amount of light entering the different maxima is a significant factor.

It is possible to assume that a third order vortex would provide even better filtering. Unfortunately, the third order maxima were quite faint, and the third order vortex

was much distorted, so I did not think it possible to get any good experimental data to resolve the issue. Theory seems to indicate that moving to the third order, or higher, vortex beam could be beneficial: the higher the topological charge, the larger the dark spot in the vortex beam. However, there are practical considerations. The hologram cannot be used for the actual filter; we must use a phase plate. For a higher order vortex, one needs either more "stair-steps", or a larger phase shift per stair-step. More stair steps are more difficult to machine, and the manufacture of spiral phase plates is a difficult process. Larger phase shifts per stair-step decreases the quality of the vortices generated, which is counter-productive. So it could be very difficult to get a spiral phase plate capable of generating vortices of order higher than two.

XIII. Experimental Determination of Coronagraph Resolution

In order to measure the resolution of the optical vortex coronagraph, I designed and constructed the apparatus shown as Figure 15. An initial picture is taken with the beam aligned with the phase mask and the pinhole, so as to maximize the filtering of the beam. I then slightly misaligned the apparatus and took a picture. This last step was repeated many times over. Then, by comparing the intensity of light passed through the pinhole for a misaligned picture with the light passed in the aligned case, the ability of the coronagraph to resolve a probe and control field at the angle of the misaligned beam from the aligned beam can be determined. Using this method I determined that the coronagraph should be capable of resolving two beams of equal intensity. with approxi-

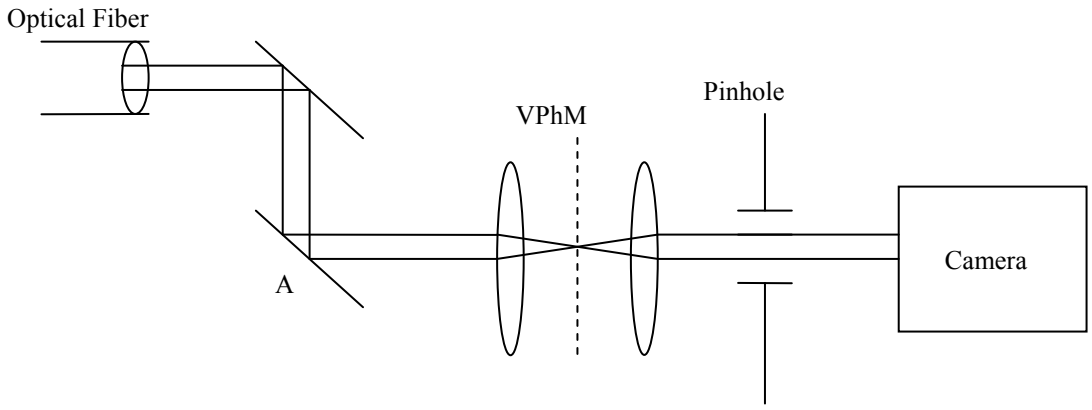

FIGURE 15: Apparatus used in attempt to measure resolution of the coronagraph. Mirror A was adjusted to misalign the laser with the phase mask, and the detected light compared with data taken when the laser

mately 1 microradian of angle between them. How this would scale to beams five orders of magnitude in intensity is unknown.

XIV. Proposed Improvements to Optical Vortex Coronagraph

The most immediate way we could improve the coronagraph would be by using second-order vortices instead of first order ones. While this would require a new phase mask and realignment, the overall arrangement would otherwise be the same, and, as the experiments with the hologram suggest, this would significantly improve filtering. I have devised two additional proposals which drastically alter the optical vortex coronagraph design, but could potentially be used to dramatically improve performance. The first would be to place the entire coronagraph in a cavity so that the light is run through the filter many times over. By running the vortex through a second phase mask, or reflecting it back through the first one, the vortex could be turned back into a Gaussian beam, before being turned into a vortex again and re-filtered. This would be very diffi-

cult to align, and would likely require extremely high beam qualities, which would be difficult with the diode lasers we currently use, but could potentially be very powerful.

The other proposal could completely eliminate the need to have a small angle between the control and probe field while sending them through the Rubidium gas cell. If a prism made of highly dispersive glass were placed after the slow light experiment but before the filter, the control and probe fields could have a very small angle of separation placed on them by the glass. A diagram of this proposal is shown as Figure 19. For practical distances away from the prism, the two fields would still not be separable due to the diffraction limit, but the optical vortex coronagraph gives us a limited ability to defeat the diffraction limit. Initial order of magnitude calculations using optical properties of the types of glass listed on the Schott Corporation's website [4] and the Sellmeier equation, shown as Equation 9,

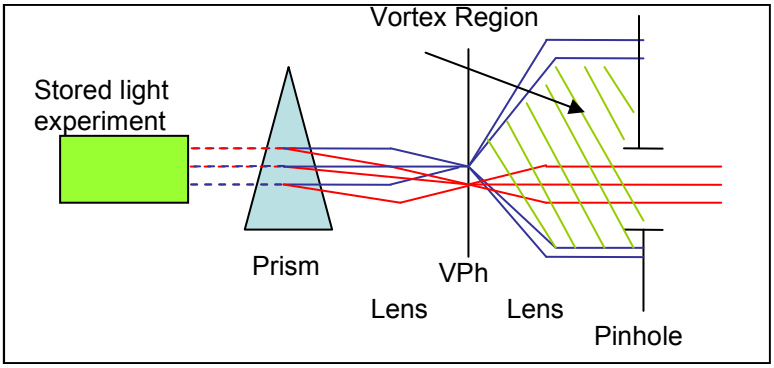

FIGURE 16: Adding a prism to the optical vortex coronagraph. The light passes through the slow light experiment completely collinearly, and is separated by a highly dispersive prism on the other side. These separated beams then enter the coronagraph.

$$n^2(\lambda) = 1 + \frac{B_1\lambda^2}{\lambda^2 - C_1} + \frac{B_2\lambda^2}{\lambda^2 - C_2} + \frac{B_3\lambda^2}{\lambda^2 - C_3} + \ldots \qquad (8)$$

Where n is index of refraction, λ is wavelength in microns, and B_x and C_x are properties of the glass given by the catalog, indicates a separation of 0.1 microradians, too small to be resolved with an optical vortex coronagraph. In order to increase the divergence cre-

ated by the prism, I am currently considering the possibility of placing the prism within a slightly misaligned optical cavity, so that the beams are sent through the prism multiple times. Initial calculations indicate that this could increase the separation between the beams by a few orders of magnitude, thought not enough to make the difference detectable. I am optimistic, however, that a thorough calculation may indicate that in fact this system could be effective, or, if not, that further improvements to the prism and cavity system could result in a useful divergence.

XV Conclusion

Experimentation with the prototype optical vortex coronagraph indicates that the device is capable of improving contrast between the probe and control field by three order of magnitude for the proper selection of design parameters. Initial tests on the stored light experiment under unideal conditions have achieved two order of magnitude. These parameters are a 3.2mm diameter probe field, a 2.4 mm diameter probe field, and 0.5 mm diameter pinhole. It is also shown that with use of a second order vortex phase mask, this could likely be improved further. Shortly, we should have results for the effectiveness of the optical vortex coronagraph at filtering the output of the stored light experiment. Should the gain in contrast not be as high as desired, the effectiveness could likely be further improved by placing the filter within a ring cavity or using a prism and cavity system to increase the beam separation.

XVI References

1. Nathan Belcher, Eugeniy E. Mikhailov, and Irina Novikova,

"Atomic Clocks and Coherent Population Trapping: Experiments for Undergraduate Laboratories"
arXiv:0810.2071v1 [physics.ed-ph]

2. Gregory Foo, David M. Palacios, and Grover A. Swartzlander, Jr**,**
"Optical vortex coronagraph"
Opt. Lett. **30**, 3308-3310 (2005)

3. Sharon A. Kennedy, Matthew J. Szabo, Hilary Teslow, James Z. Porterfield, and E. R. I. Abraham,
"Creation of Laguerre-Gaussian laser modes using diffractive optics"
Physical Review A **66**, 43801-1-43801-5 (2002)

4. Schott Inc.
"Optical Glass Datasheetsv170309"
Schott Incorporated http://www.us.schott.com/advanced_optics/english/tools_downloads/download/index.html#Catalogues%20and%20Datasheets

5. Z.S. Sacks, D. Rozas, and G.A. Swartzlander, Jr.,
"Holographic Formation of Optical-Vortex Filaments"
J. Opt. Soc. Am. B, **15**, 2226-2234 (1998)

6. Zhongyi Guo, Shiliang Qu, and Shutian Liu,
"Generating optical vortex with computer-generated hologram fabricated inside glass by femtosecond laser pulses"
Opt. Commun. **273** p. 286 (2006),

7. David M. Palacios
"An Optical Vortex Coherence Filter"
2004, Available at:
http://www.wpi.edu/Pubs/ETD/Available/etd-0824104-123434/unrestricted/palacios.pdf

8. David Palacios, David Rozas, and Grover A. Swartzlander, Jr.
"Observed Scattering into a Dark Optical Vortex Core"
Phys. Rev. Lett., **88**, 103902, 1-4 (2002)

9. Amol Jain
"Creation of Optical Vortices Using an Adjustable Spiral Phase Plate and Computer Generated Holograms"
Retrieved from http://laser.physics.sunysb.edu/~amol/papers/siemens/siemens.pdf

10. K. T. Gahagan and G. A. Swartzlander Jr.
"Optical Vortex Trapping of Particles"
Optics Letters, **21**, 827-829 (1996)

11. Absolute Astronomy
"Electromagnetically Induced Transparency"
Absolute Astronomy
http://www.absoluteastronomy.com/topics/Electromagnetically_induced_transparency